X-613-66-451

55676

MEASUREMENTS OF INTERPLANETARY DUST PARTICLE FLUX FROM EXPLORER XVI CdS AND WIRE GRID DUST PARTICLE DETECTORS

BY

LUC SECRETAN

SEPTEMBER 1966

NASA — GODDARD SPACE FLIGHT CENTER —

GREENBELT, MD.

X-613-66-451

MEASUREMENTS OF INTERPLANETARY DUST PARTICLE FLUX FROM EXPLORER XVI CdS AND WIRE GRID DUST PARTICLE DETECTORS

By

Luc Secretan

GODDARD SPACE FLIGHT CENTER
GREENBELT, MARYLAND

NATIONAL AERONAUTICS AND SPACE ADMINISTRATION

CONTENTS

ABSTRACT

The CdS dust particle detectors on Explorer XVI provide a means of determining the flux of dust particles in the vicinity of the earth, by measuring the area of the perforations due to impacts of dust particles of mass $\geq 10^{-10}$ gm through a 1/4 mil aluminized mylar film.

One CdS detector measured a total area of 0.08 mm^2 perforated by dust particles over a 55-day period; the other measured an area of 0.0068 mm^2 in 20 days. The perforated area is proportional to the cumulative flux of impacting particles of mass $\geq 10^{-10}$ gm.

The flux measured by the detectors is compared with several models provided by other satellite observations and various ground based observations. When the flux model derived from direct satellite measurements is used, ($\log I = -17 - 1.7 \log M$, where I is the cumulative influx rate and M is the mass of the particles) it is found that approximately 10^3 impacts would occur. The area opened up by these impacts is in excellent agreement with the results of the CdS detector experiment. Flux models derived from ground based observations predict too few impacts for the mass range of particles considered here.

A second dust particle experiment employed a wire grid sensor which would detect particles of mass 10^{-7} gm and larger. Two wires were broken. This is in good agreement with the dust particle flux model derived from direct satellite measurements.

MEASUREMENTS OF INTERPLANETARY DUST PARTICLE FLUX FROM EXPLORER XVI CdS AND WIRE GRID DUST PARTICLE DETECTORS*

by

Luc Secretan
Goddard Space Flight Center

INTRODUCTION

Explorer XVI (Figure 1) was designed essentially to assess the micrometeoroid hazard to thin sheet metal exposed in space. Two other experiments were added in the form of wire grids and a mylar covered CdS photoconductor. This paper describes these two experiments and analyzes the resulting data.

Explorer XVI was the third satellite in a series of three launched by the Scout S55 vehicle. The first launch failed. The second partially failed without providing data, but the satellite was aloft long enough to show a defect in the design of the CdS detector. This was corrected and the detector, which will be described presently, operated normally in Explorer XVI. Explorer XVI, launched on December 16, 1962, had twin telemetry systems: A and B. System A operated normally until May 29, 1963; B operated until July 25, 1963. Reference 1 gives a report on all the experiments for the first 28 days of 221 days of satellite operation. The wire grid experiment and the CdS experiment are described in the pages that follow. No attempt is made to compare these with the other experiments aboard the satellite.

DESCRIPTION OF THE TWO SENSORS

THE CdS CELLS

The design of the Explorer XVI CdS sensors was derived from the original design used successfully on Vanguard III, 1959η (Reference 2) and on Explorer VII, 1959ι1 (Reference 3). Figure 2 shows a cross section, with the mylar stretched

*Given at the Symposium on Meteor Orbits and Dust, Boston, Mass., August 9–13, 1965.

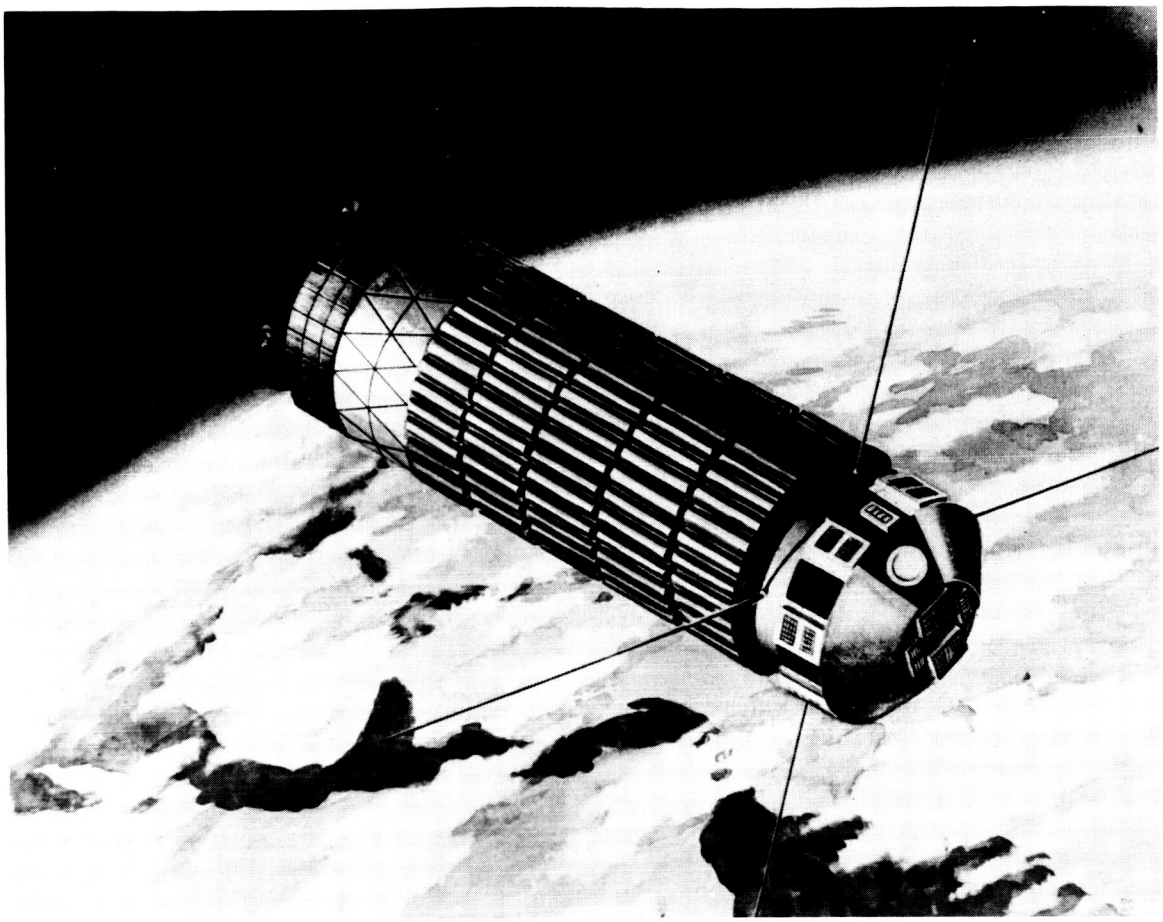

Figure 1 – Explorer XVI.

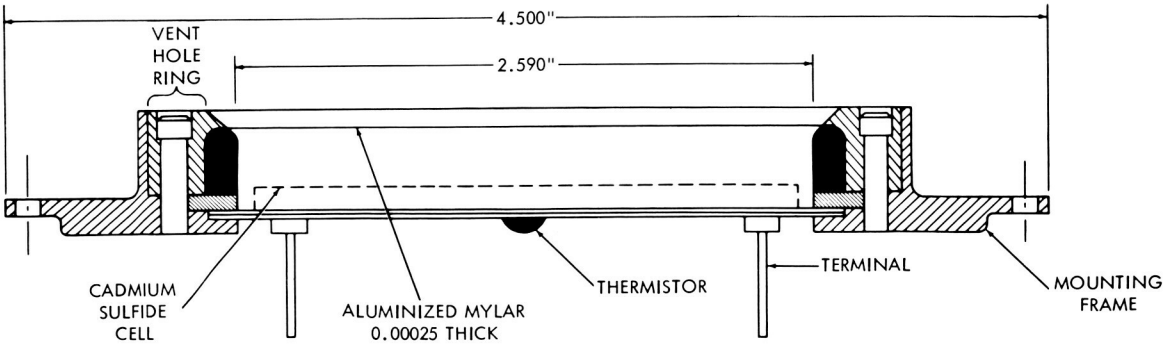

Figure 2 – The CdS cell.

Figure 3 – Ring showing the vent holes for the CdS cell.

across the face of the cell. Vent holes (Figure 3) are designed to provide large air passages without permitting sunlight to reach the sensitive cell.

The mylar film covering the cells was coated on both sides with aluminum in order to provide absolute opacity and to assure that any light input would be caused by perforation and not by surface erosion or flaking. There is one cell for each telemetry system. Each cell has an effective area of $2 \times 10^{-3}\,m^2$. The mylar film of Cell A was left completely opaque, while the film of Cell B was perforated with a nominal 0.002 inch hole for inflight calibration purposes. In orbit the initial resistance of Cell B dropped to a value near 40 K ohms, which showed that the system started operating as expected with a solar aspect angle of 30° from the normal. During the lifetime of the experiment, this aspect angle was 30° or less.

THE COPPER WIRE GRIDS

The wire-wound cards are shown in Figure 4 and their dimensions given in Table 1. Reference 1 describes the wire grid experiment in detail.

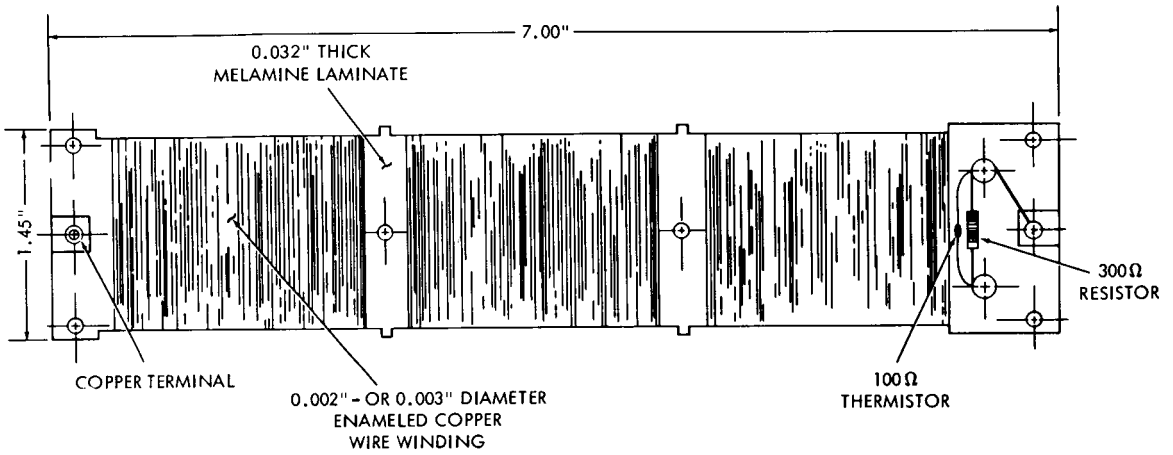

Figure 4 – The copper wire card detector.

Table 1

Wire Thicknesses and the Areas of the Wire Cards.

Diameter of Wire		Number of Sensors	Area/Sensor (ft^2)	Total Exposed Area*	
(in.)	(Microns)			(ft^2)	(m^2)
0.002	50	14	0.0474	0.664	6.1×10^{-2}
0.003	75	32	0.0948	1.517	14.1×10^{-2}

* Total exposed Area = 20.2×10^{-2} m^2 = 0.2 m^2

CALIBRATION OF DETECTORS

THE CdS PHOTOCONDUCTORS

About a dozen CdS cells were tested and calibrated in order to find two with nearly equal sensitivity to light inputs. Calibration established the change of resistance of each cell for a given light input through calibrated pinholes, and those cells with the most uniform light sensitivity across the entire surface were selected. Figure 5 shows the calibration curve for the two cells in orbit. A line

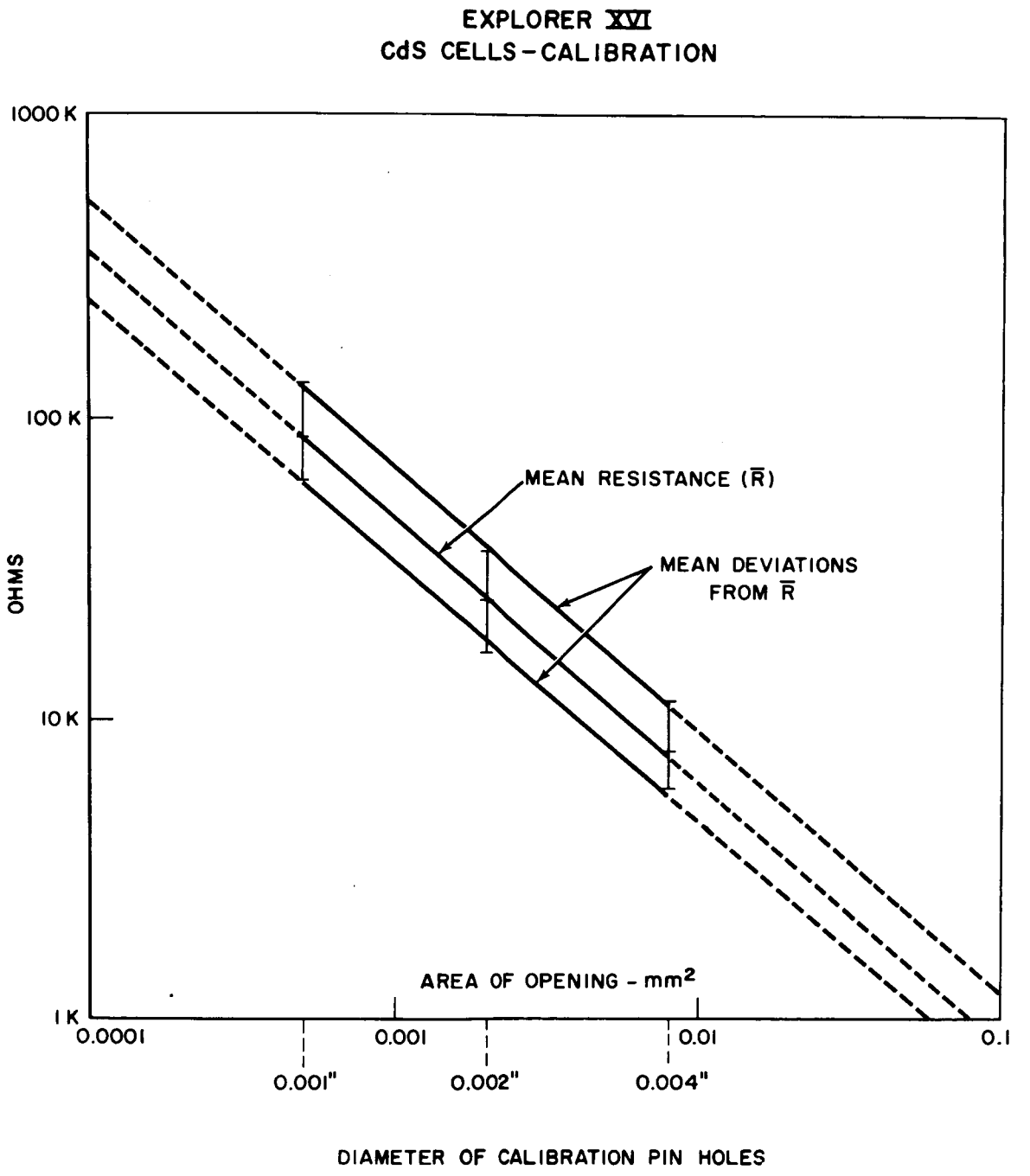

Figure 5 – Calibration of Explorer XVI CdS cells.

drawn through the mean values obtained when rotating the cell for 5 minutes in a xenon arc beam has been used to evaluate the telemetered resistance data.

Preliminary tests established the correlation between the light intensity of the xenon arc and that of the sun. The scatter in the data for Figure 5 represents the variation in sensitivity over the complete area of the cell established by the positioning of single pinholes during calibration. Laboratory calibrations established the cumulative characteristics of the detector. Since in flight the detector measures the cumulative area of many necessarily random perforations, the resistance value for a large number of holes approaches the mean value shown in Figure 5. The relation between particle size and perforated hole diameter in 1/4 mil mylar has been established in the laboratory by Friichtenicht (Reference 4) and independently by the author. For iron particles, the density $\rho = 7.8$ gm/cm^3 and the hole size is 1 to 1.5 times larger than the penetrating particle.

The CdS cells were calibrated with respect to temperature, and a linear relation between resistance and temperature was determined for the expected operating thermal range.

WIRE GRID THERMO-ELECTRIC COMPENSATION

The copper wire grids were temperature-compensated for resistance changes, which were not to exceed 3% between -20°C and +60°C. Figure 6 shows the circuit of the 21 TE5 compensating thermistor and associated wire grids. The resulting resistance curves for 0.003 inch and 0.002 inch wires are compared with a curve for uncompensated wire.

RESULTS OF THE CdS CELL AND WIRE GRID EXPERIMENTS

Processed data from the two experiments were received in the following form:

1. Resistance of Cells A and B (ohms);
2. Temperature of Cells A and B (°C);
3. Information indicating either continuity or breakage of a wire on one or more cards; and
4. Length of interrogation, date, and station.

The resistance data were normalized to the launch temperature of the cells (35°C) by means of the empirical linear relation between temperature and resistance: $R_t = R_{35} + K\,(t - T_{35})$, where K = 660 ohms and t is the cell temperature in °C.

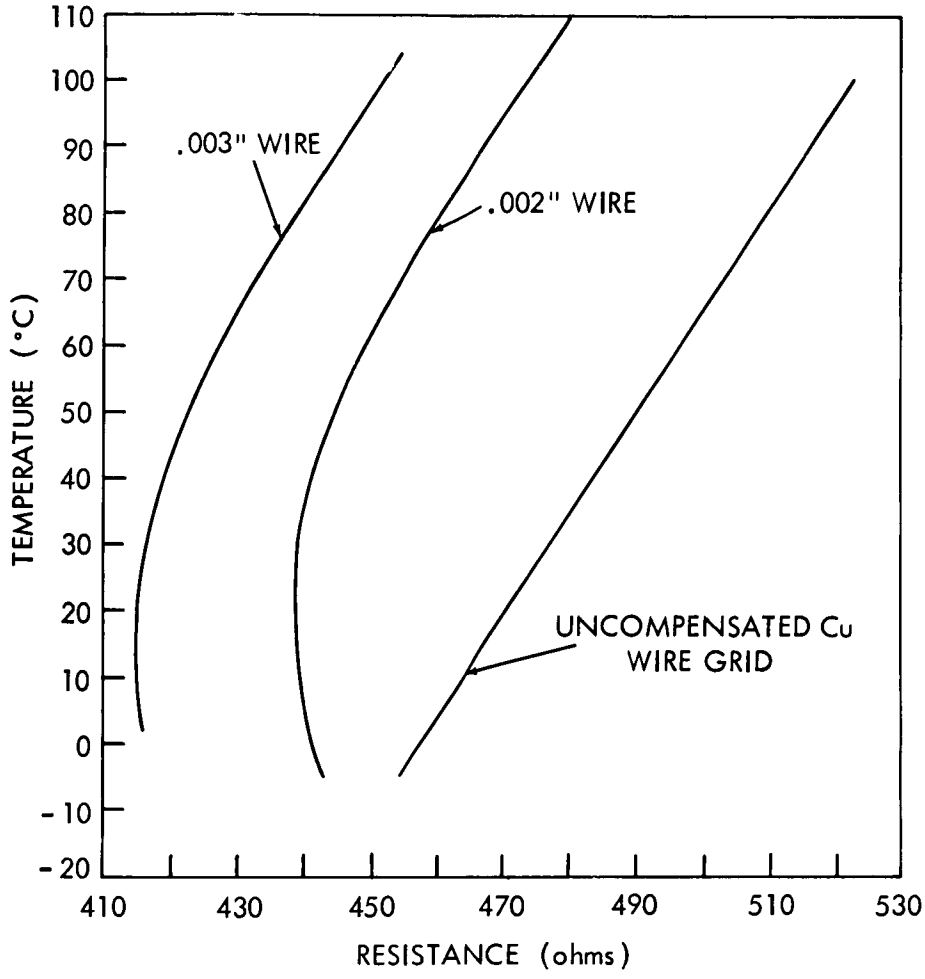

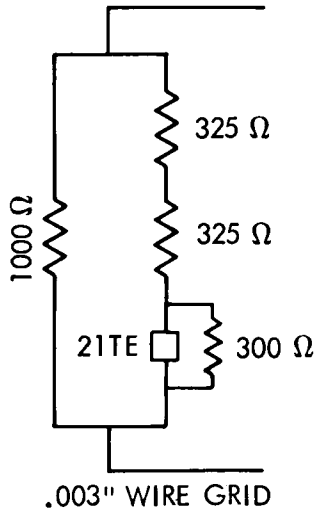

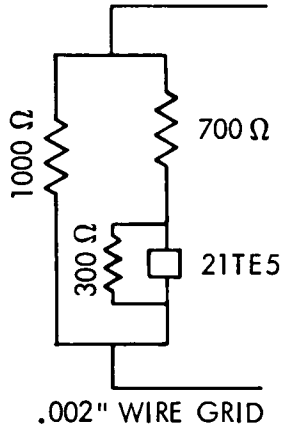

Figure 6 – Thermo-electric compensation of copper wire grids.

This thermal relation remained valid for Cell B until December 31, 1962. After this data the temperature correlation changed and it became impossible to establish a relation between resistance and hole size. For Cell A the case was more favorable and the data could be followed to February 5, 1963 when, as a result of successive perforations, the minimum recordable resistance was obtained.

Changes of aspect to the sun have been considered. After 55 days the sensor aspect is the same as at launch time, owing to the geometry of the orbiting vehicle. The data are interpreted in terms of cumulative perforated areas. Intermediate changes shown are affected by an aspect uncertainty factor of two.

A simplified diagram of the compensated CdS data is shown in Figure 7. Cell A remained dark at about 300 K ohms until 2 days after launch. The first indication of light penetration was on December 18, 1962, when the cell showed a decrease in resistance. On December 23, 1962, the first marked event happened. The cell was still showing darkness in twilight December 23, 1962, at 11:40, but showed a 0.002 inch hole during the next pass at 12:30. Further measurements of perforated areas of Cells A and B occurred, as may be seen from Tables 2 and 3.

The wire grids were monitored for the lifetime of the satellite. Two breaks occurred, one of the 3 mil and one of the 2 mil wire.

Owing to the satellite's rotation with respect to the sun, the resistance of the cell is lowest when the sun's rays are normal to the mylar film. For this reason the lowest resistance readings have been considered exclusively as data points in evaluating the size of the perforations. Dates of those readings and the estimated additional cumulative perforated areas are given in chronological order in Tables 2 and 3. It must be emphasized that the data in Tables 2 and 3 do not represent discrete events but cumulative status read-outs when the satellite was in a suitable position both as to orbit and solar aspect.

DATA ANALYSIS

The CdS cell detectors measured the cumulative perforated area caused by in-flight impacts on the mylar by dust particles. As was previously stated, the accuracy of the measurements increases with the number of perforations. Therefore, the method of analysis applied in this paper is as follows:

1. Hypervelocity micro particle impact experiments in the laboratory show that the threshold mass of the perforating particles is approximately 10^{-10} gm for the denser particles and 10^{-9} gm for the less dense ones. The diameter of the hole in mylar is 1 to 1.5 times the diameter of the perforating particle, allowance being made for the range of specific gravity of the impacting particles.

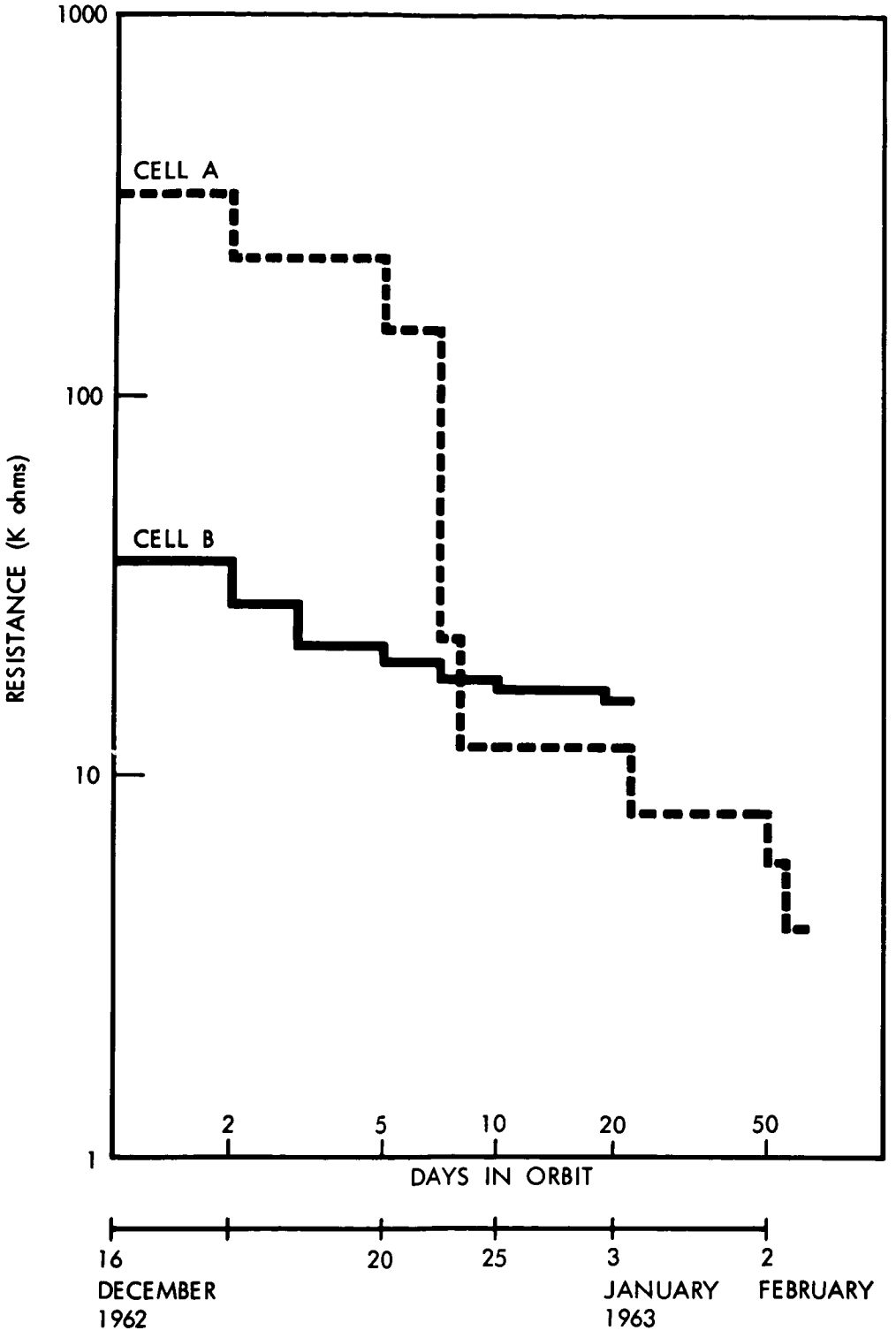

Figure 7 – Drop of resistance of cells A and B with time in orbit.

Table 2
Cell A Data Compensated to 35°C for a 55 Day Period.

Date	Cumulative Time (days)	Hole Area (mm^2)	
		Total Area	Additional Perforated Area
December 16		0	0
December 18	2	.00015	.00015
December 21	5	.00024	.00009
December 23	7	.0020	.00178
December 24	8	.011	.009
January 7	22	.023	.012
February 4	50	.033	.010
February 9	55	.080	.047
Total additional area			.080

Table 3
Cell B Data Compensated to 35°C for a 20 Day Period.

Date	Cumulative Time (days)	Hole Area (mm^2)	
		Total Area	Additional Perforated Area
December 16-17		.0012	0
December 18	2	.0016	.0004
December 19	3	.0020	.0004
December 21	5	.0022	.0002
December 23	7	.0025	.0003
December 26	10	.0065	.0040
January 4	19	.0080	.0015
Total additional area			.0068

2. It is considered that the total perforated area is caused by particles of mass near the threshold limit of the detector.

3. A model for the cumulative flux distribution of dust particles in the vicinity of the earth is assumed in order to compute an expected rate of perforation.

4. Finally, the expected cumulative area of perforations is compared with the data.

5. Because of uncertainties in aspect and thermal corrections, the expected accuracy of the cumulative perforated areas is limited to a factor of 2.

The computations were carried out on the basis of:

(1) A cumulative flux mass distribution model given by

$$\text{Log } I = -17 - 1.7 \log M,$$

(Equation 1 of Reference 5);

(2) Three different mass threshold sensitivities:

$$10^{-10},\ 10^{-9},\ 10^{-8} \text{ gm};$$

(3) Three different possible densities of particles, i.e.

$$\rho_1 = 1 \text{ gm/cm}^3 \text{ (ice)}$$

$$\rho_2 = 4 \text{ gm/cm}^3 \text{ (stone)}$$

$$\rho_3 = 8 \text{ gm/cm}^3 \text{ (iron)}$$

The expected cumulative perforated areas as a function of time for masses 10^{-10}, 10^{-9}, 10^{-8} gm and densities of 1, 4, and 8 gm/cm^3 have been computed using Equation 1 of Reference 5 (Tables 4, 5, 6, and 7).

Data from cell A showed a cumulative perforated area of 0.08 mm^2 for the 55-day experiment. The expected cumulative area for 10^{-10} gm particles (Table 7) varies from 0.055 to 0.143 mm as the specific gravity is varied from 4 to 1. Table 7 gives similar information concerning cell B.

Table 4

Area of One (1) Hole in Mylar.

	Mass = 1 x 10^{-10} gm/cm^3			Mass = 1 x 10^{-9} gm/cm^3			Mass = 1 x 10^{-8} gm/cm^3		
Density of Particle (gm/cm^3)	$\rho = 1$	$\rho = 4$	$\rho = 8$	$\rho = 1$	$\rho = 4$	$\rho = 8$	$\rho = 1$	$\rho = 4$	$\rho = 8$
Diameter of Particle (μ)	5.8	3.6	2.9	12.4	7.9	6.2	26.9	16.9	13.7
Diameter of Hole (mm)	.0087	.0054	.0044	.0189	.0119	.0095	.0404	.0254	.0206
Area of Hole (mm^2)	5.9×10^{-5}	2.3×10^{-5}	1.5×10^{-5}	2.8×10^{-4}	1.1×10^{-4}	7.1×10^{-5}	12.8×10^{-4}	5.1×10^{-4}	3.3×10^{-4}

Table 5

Cumulative Flux

Log I = -17 - 1.70 Log M.

Log M	I (impacts/m^2 - sec)
-10	1×10^{0}
- 9	$1 \times 10^{-1.7}$
- 8	$1 \times 10^{-3.4}$

Table 6

Impacts per Day.

MASS (gm)	PARTICLE INFLUX (impacts/m^2 - sec)	SENSOR AREA (m^2)	AREA x TIME (m^2 - sec)	IMPACTS PER DAY
10^{-10}	1 x 10^{0} or 1	2 x 10^{-3}	1.73 x 10^{2} m^2 sec	1.73 x 10^{2}
10^{-9}	1 x $10^{-1.7}$	2 x 10^{-3}	1.73 x 10^{2} m^2 sec	3.45
10^{-8}	1 x $10^{-3.4}$	2 x 10^{-3}	1.73 x 10^{2} m^2 sec	6.91 x 10^{-2}

Table 7

Expected Cumulative Perforated Areas for Particles of Various Specific Gravities.

Particle Mass (gm)	Specific gravity	Expected-Cumulative Perforated Areas (mm^2)	
		20 days (Cell B)	55 days (Cell A)
1 x 10^{-10}	1	5.2 x 10^{-2}	1.43 x 10^{-1}
	4	2.0 x 10^{-2}	5.5 x 10^{-2}
	8	1.2 x 10^{-2}	3.6 x 10^{-2}
1 x 10^{-9}	1	4.8 x 10^{-3}	1.32 x 10^{-2}
	4	1.9 x 10^{-3}	5.2 x 10^{-3}
	8	1.2 x 10^{-3}	3.4 x 10^{-3}
1 x 10^{-8}	1	4.4 x 10^{-4}	1.21 x 10^{-3}
	4	1.7 x 10^{-4}	4.8 x 10^{-4}
	8	1.1 x 10^{-4}	3.1 x 10^{-4}

CONCLUSION

The data from the mylar-CdS experiment described in this paper are interpreted as due to perforations through an opaque cover by microparticles in the vicinity of the earth.

If the cumulative flux (Reference 5), is used as a guideline, good agreement is obtained for densities ranging from 1 to 4 gm/cm^3.

Within the framework of our assumptions concerning the physical parameters of the particles and sensor threshold sensitivity, the particles detected in this experiment were predominantly in the mass range of 10^{-10} and 10^{-9} gm for densities between 1 and 4 gm/cm^3.

The wire grid experiment confirms the above statement for masses of the order of 10^{-7} gm, of probably higher densities.

Appendix A shows that Equation 1 (Reference 5) predicts six impacts, while only two have been observed.

A discussion follows on the possibility of erosion of the front coating of the mylar film.

DISCUSSION OF RESULTS

In the course of the discussion at this symposium on the results of the CdS experiment, Professor Whipple pointed out that the drop of resistance of the CdS cells may have been due to transparency of the mylar film coating or to pinholes, if the total area had been eroded.

The experiments on Vanguard III and on Explorer VII have proved conclusively that the front film did not erode completely; the cells remained "dark".

Regarding the transparency of the back film, the following experiment has been performed with a spare film fabricated at the same time (and by the same people) as the flight films.

1. The front aluminum coating was completely etched away.

2. The mylar film was then placed on a CdS cell of the same type as the flight unit.

3. A strong light spot 1 cm in diameter was focused on the cell, and a reading was obtained.

4. The same arrangement was repeated, using a brass plate perforated by a pinhole .0025 cm in diameter. The same reading was obtained as with the 1 cm etched mylar film. The ratio of areas is roughly 2×10^5. The flux required to erode an equivalent area would be 5 orders of magnitude greater and the particle mass would be on the order of 10^{-14} gm. The size of these particles would be in the range of 1000 Angstroms. Owing to radiation pressure effects, it is improbable that such particles exist in the vicinity of earth.

Appendix A

Micrometeoroid Impacts on Wire Grids

By using Equation 1 of reference 5, we can compute the number N of impacts for the wire-wound sensors. Let the particle with a diameter of 60 μ and a density of 1 gm/cm^3 be the mass (M = 10^{-7} gm) that would break the copper wires used; then

$$\log I = -17 - 1.7 \log M,$$

$$= -5,$$

$$I = 1 \times 10^{-5} \text{ impacts/m}^2\text{-sec.}$$

Since $AT = 62 \times 10^4$ m^2 sec, where A = area and T = time

$$N = ATI = 62 \times 10^4 \times 10^{-5}$$

$$= 6.2 \text{ impacts.}$$

This value compares favorably with experimental results, which show two broken wires. In considering the impacts upon the wire-wound grids, we see that the wires will not always be hit head-on (i.e., the particles may graze the wire or merely penetrate the insulation which surrounds each wire.)

If the above calculation is performed for particles with M = 10^{-6} gm, then N = 0.1 impact. Therefore, since the actual number of impacts must be greater than the number recorded (i.e., not all of the micrometeoroids will hit the wires head-on), the particles detected by the wire grids are of the order of 10^{-7} gm or larger.

REFERENCES

1. Hastings, E. C., Jr., "The Explorer XVI Micrometeoroid Satellite." NASA Technical Memorandum X-810, February 1963.

2. LaGow, H. E., Secretan, L., and Giuliani, J., "Experiments for Satellite Environmental Measurements," presented at the IGY Rocket and Satellite Conference, Washington, D. C., September 30 - October 5, 1957; in Annals of the International Geophysical Year, Vol. IV, Parts I-V, New York: Pergamon Press, 1958, pp. 319-321.

3. LaGow, H. E., and Secretan, L., "Results of Micrometeorite Penetration Experiment on the Explorer VII Satellite (1959 Iota)," NASA Technical Note D-1722, April 1963.

4. Friichtenicht, J. F., "Study of Crater Physics," Report No. 3, Space Technology Labs., Ramo Wooldridge Inc., July 1961.

5. Alexander, W. M., McCracken, C. W., Secretan, L., and Berg, O. E., "Review of Direct Measurements of Interplanetary Dust from Satellites and Probes" in Space Research III, ed. by W. Priester. Amsterdam: North-Holland, 1963, pp. 891 - 917.

6. Whipple, F. L., "On Meteoroids and Penetration," J. Geophys. Res. 68 (17): 4929-4947, September 1, 1963.